Effects of Lesion Size and Location on Equine Articular Cartilage Repair

Mark B. Hurtig, Peter B. Fretz, Cecil E. Doige and Dan L. Schnurr*

ABSTRACT

The mechanisms and completeness of equine articular cartilage repair were studied in ten horses over a nine month period. Large (15 mm square) and small (5 mm square) full-thickness lesions were made in weight bearing and nonweight bearing areas of the radiocarpal, middle carpal and femoropatellar joints. The horses were euthanized in groups of two 1, 2.5, 4, 5 and 9 months later. Gross pathology, microradiography, and histopathology were used to evaluate qualitative aspects of articular repair. Computer assisted microdensitometry of safranin-O stained cartilage sections was used to quantitate cartilage matrix proteoglycan levels.

Structural repair had occurred in most small defects at the end of nine months by a combination of matrix flow and extrinsic repair mechanisms. Elaboration of matrix proteoglycans was not complete at this time. Statistically better healing occurred in small weight bearing lesions, compared to large or nonweight bearing lesions. Synovial and perichondrial pannus interfered with healing of osteochondral defects that were adjacent to the cranial rim of the third carpal bone. Clinical and experimental experience suggests that these lesions are unlikely to heal, whereas similar lesions in the radiocarpal and femoropatellar joints had satisfactory outcomes. Observations made in this study support the use of early postoperative ambulation, passive flexion of operated joints, and recuperative periods of up to a year for large cartilage defects.

RÉSUMÉ

Cette expérience portait sur dix chevaux et elle visait à étudier les mécanismes et l'intégralité de la réparation de leurs cartilages articulaires, sur une période de neuf mois. Les auteurs provoquèrent à cette fin des entailles qui impliquaient toute l'épaisseur de certains cartilages des articulations radio-carpiennes, carpiennes médiales et fémoro-patellaires, supporteurs ou non du poids; ces entailles mesuraient 15 mm^2 ou 5 m^2. Ils sacrifièrent ensuite deux chevaux à la fois, au bout d'un, 2,5, quatre, cinq et neuf mois. Ils basèrent leur évaluation des aspects qualitatifs de la réparation articulaire, sur les lésions macroscopiques, la microradiographie et l'histopathologie. Ils utilisèrent la microdensitométrie de sections de cartilages, colorées à la safranine-O, assistée d'un ordinateur, pour quantifier la teneur de la matrice cartilagineuse en protéoglycane.

Au bout de neuf mois, la plupart des petites lésions affichaient une réparation structurale complète, grâce à la synergie du flux de la matrice et de la réparation extrinsèque; l'élaboration des protéoglycanes de la matrice n'était toutefois pas complète. Du point de vue statistique, une meilleure réparation se produisit dans les petites lésions qui subissaient la pression du poids que dans les grandes qui ne la subissaient pas. Le pannus synovial et périchondral fit échec à la guérison des lésions ostéochondrales, adjacentes à la partie crâniale du pourtour du troisième os carpien. L'expérience clinique et expérimentale laisse croire que ces lésions ne guérissent à peu près pas, contrairement à des lésions semblables des articulations radio-carpiennes et fémoro-patellaires. Les observations enregistrées au cours de cette étude appuient l'utilisation de la marche, tôt après la chirurgie, de la flexion passive des articulations opérées et de périodes de récupération qui peuvent aller jusqu'à un an, pour les lésions importantes des cartilages.

INTRODUCTION

Developmental disorders such as osteochondritis dessicans, athletic injuries such as carpal fractures, and the incidence of degenerative joint disease have sustained veterinarians' interest in the horse's innate potential for articular repair. There are two mechanisms of articular cartilage repair (1,2). Intrinsic repair relies on the limited mitotic capability of the chondrocyte and a short-lived increase in metabolic products, (chiefly collagen and proteoglycans). Extrinsic healing relies on mesenchymal elements from subchondral bone to participate in the formation of new connective tissue that later may undergo metaplastic changes to form hyaline cartilage. A third phenomenon known as "matrix flow", has been reported to contribute to cartilage repair by forming wave-like lips of

*Department of Clinical Studies, Ontario Veterinary College, University of Guelph, Guelph, Ontario N1G 2W1 (Hurtig, Schnurr), Department of Veterinary Anesthesia, Radiology and Surgery (Fretz) and Department of Veterinary Pathology (Doige), Western College of Veterinary Medicine, University of Saskatchewan, Saskatoon, Saskatchewan S7N 0W0.

Funding for this study was provided by the Western College of Veterinary Medicine Equine Health Research Fund and the Guelph Centre for Equine Research.

Submitted June 5, 1987.

cartilage from perimeter of the lesion that migrate toward the center of the defect (1-4).

While there are reports of complete hyaline cartilage repair (4,5), most observers agree that a surface of somewhat lesser quality than hyaline cartilage results from the healing offull thickness defects in all species studied to date (3,6,7). Nevertheless some articular lesions are associated with a very good prognosis while others are not (McIlwraith CW, personal communication, 1986). Surgeons have attempted to correlate lesion size and anatomical location with prognosis in naturally occurring equine joint disease but there are few reports of this type of investigation carried out under controlled conditions (8,9).

The qualitative assessment of cartilage healing is problematic and has been considered somewhat arbitrary and imprecise (5). Several authors have attempted to grade or score the cellular events and organization that take place in healing articular cartilage, but these classifications lack precision (10). Visual assessment of metachromatic or orthochromatic staining has been used as an indicator of matrix proteoglycan concentration and healing, but differences in tissue processing and staining technique render this methodology unreliable (11). Recent reports using microdensitometry for measurement of matrix proteoglycans in specially stained safranin-O stained sections of articular cartilage have shown that the method is both specific and stochiometric with respect to quantitation of cartilage proteoglycans (10,11).

This study was designed to investigate the mechanisms and completeness of equine articular repair by both qualitative scoring and quantitative microdensitometry. The effects of lesion size and anatomical location on articular repair were examined to help establish prognostic features in naturally occurring joint disease.

MATERIALS AND METHODS

Ten adult crossbred horses between two and five years of age were selected at a local auction on the basis of their temperament and musculoskeletal soundness. The horses were divided into five groups of two and housed in boxstalls during a conditioning period of two weeks. They were dewormed, and given tetanus toxoid, equine influenza and rhinopneumonitis vaccines. Four standard radiographic views of each carpus (lateral to medial, cranial to caudal, cranial to caudal medial oblique and cranial to caudal lateral oblique) and two views of each stifle (lateral to medial, caudal to cranial) were taken to rule out occult articular lesions.

EXPERIMENTAL DESIGN AND SURGICAL TECHNIQUE

The ten horses underwent arthroscopic surgery to create one full-thickness defect in each of the radiocarpal, middle carpal and femoropatellar joints. A repeating block design equally assigned two variables to lesions in the sixty joints (Table I). There were two possible sizes for lesions (small or large), and two possible locations (weight bearing or nonweight bearing). Small lesions were 5 mm square and large lesions were 15 mm square. Central, weight bearing lesions were created on concave portions of the radial and third carpal bones 1.5 cm from the cranial rim of the joint. Central femoropatellar lesions were made at the junction of the lateral trochlea and trochlear groove in an area directly contacted by the patella. Nonweight bearing lesions were made on the rounded cranial rim of the radial and third carpal bones, and high on the axial side of the lateral trochlear ridge of the femur not contacted by the patella. The four treatments were randomly assigned across time and horses (Table I).

The lesions were created after anesthetic induction with intravenous thiamylal (4.4 mg/kg) and glyceryl guiacolate (100 mg/kg). Anesthesia was maintained by halothane delivered through a cuffed endotracheal tube in a semiclosed system. The horses were positioned in right lateral recumbency on a padded surgery table. The left carpus and stifle were prepared and draped for aseptic surgery. A 4.5 mm diagnostic arthroscope was inserted into the radiocarpal joint through a lateral approach and the synovial space was examined for abnormalities using a previously reported technique (12). An arthroscopic hook probe with millimeter markings was inserted through a medial approach and used to inscribe a 5 mm (small) or 15 mm (large) square on the surface of the radial carpal bone. The cartilage contained within the outline was removed with a motorized arthrotome using a 6.5 mm burr inserted through the medial approach. Brun's curettes (sizes 0 and 00) were used to remove any remaining flaps of cartilage and to expose bleeding subchondral bone. The joints were vigorously lavaged with 1 L of lactated Ringer's solution before closure of the arthroscope and instrument approach sites with one skin suture of 2-0 polypropylene each.The above protocol was repeated to create lesions on the third carpal bone of the middle carpal joint, and the trochlear groove or lateral ridge of the femoropatellar joint. The horses were then rolled into left lateral recumbency and repositioned to allow the same treatments to be carried out on the right carpus and stifle. The carpal joints were bandaged prior to

TABLE I. Allocation of Experimental Lesions to Joints of Ten Horses

	Time 1 mos		Time 2.5 mos		Time 4 mos		Time 5 mos		Time 9 mos	
	Horse		Horse		Horse		Horse		Horse	
Joint	1	2	1	2	1	2	1	2	1	2
Right radiocarpal	LC	SC	LP	SP	LC	SC	LP	SP	LC	SC
Left radiocarpal	SP	LP	SC	LC	SP	LP	SC	LC	SP	LP
Right middle carpal	LC	SC	LP	SP	LC	SC	LP	SP	LC	SC
Left middle carpal	SP	LP	SC	LC	SP	LP	SC	LC	SP	LP
Right stifle	LC	SC	LP	SP	LC	SC	LP	SP	SC	LC
Left stifle	SP	LP	SC	LC	SP	LP	SC	LC	SP	LP

LC = Large central
SC = Small central
LP = Large nonweight bearing
SP = Small nonweight bearing

the animals' recovery from anesthesia in a padded recovery stall. A single intravenous dose of 4 mg/kg of phenylbutazone was administered when the horses stood. They were returned to their boxstalls and hand walked 20 minutes twice daily during the first postoperative day and then turned out in a 10 x 10 m paddock which prevented the horses from running at gaits faster than a slow trot for the remainder of the experiment. The bandages were changed daily and then discontinued at seven days when skin sutures were removed.

TABLE II. Scoring System Used to Grade Cellular and Matrical Events in Articular Cartilage Healing

Score	Cellular Organization	Safranin-O Staining	Attachment to Subchondral Bone
0	Early fibrous and vascular elements	No matrix staining	Large clefts or unattached areas
1	Incompletely differentiated mesenchymal tissue	Slight matrix staining	Intermittent attachment
2	Organized chondrocytes in lacunae	Moderate matrix staining	Complete attachment
3	Hyaline cartilage	Normal staining	Complete attachment and reduplication of the tidemark

POSTMORTEM ASSESSMENT OF EXPERIMENTAL SITES

The ten horses were randomly divided into five groups of two which were euthanized with intravenous pentobarbitol 1, 2.5, 4, 5 and 9 months respectively after surgery. The carpal and femoropatellar joints were disarticulated and photographed. A bandsaw was used to cut serial 3 mm sagittal slabs of the healing articular surface and bone. These slabs were then imaged by microradiography (Faxitron x-ray system model 43855-A, Hewlett-Packard Inc., McMinnville, Oregon) and fixed in 10% buffered formalin for 24 hours followed by decalcification in formic acid for four days at room temperature. All the tissue slices were then trimmed, and processed routinely for histopathology. Special care was taken during embedding to ensure that the articular surface remained perpendicular to the microtome blade during sectioning. Six micron sections were cut and stained with hematoxylin and eosin (H & E), safranin-O and Masson's trichrome stain. All the safranin-O sections were stained as a batch by the same histotechnologist in an effort to standardize staining intensity.

Stained histological sections were examined qualitatively for evidence of healing. A scoring system modified from Salter *et al* (5) that emphasizes cell type and organization in healing articular cartilage was used to generate qualitative scores (Table II).

Computer assisted densitometry was used to quantitate safranin-O staining of the healing articular cartilage. A black and white video camera (Panasonic CCTV camera #WW-140, Matsushita Communications Industrial Ltd., Japan) mounted on a microscope provided images at 25 magnifications to a microcomputer (IBM personal computer, International Business Machines Corp., Armonk, New York) equipped with video interface (Video Van Gogh video digitizing circuit board and software, Tecmar Inc., Solon, Ohio) and graphics (Graphics Master graphics circuit board and software, Tecmar Inc., Solon, Ohio) circuit boards. Video images of safranin-O stained sections were digitized by the computer. The digitizing process assigned a numerical value for light transmission (luminescence) to each lighted point (pixel) on the video screen. Luminescence was inversely proportional to staining intensity which was proportional to proteoglycan concentration. A variable intensity fiber optic light source replaced the incandescent light source of the microscope to allow fine adjustments in light intensity and to eliminate background shadows from the incandescent filament. The light intensity was initially calibrated using variable resistors in the video circuit board until a clear portion of a glass microscope slide produced a light intensity reading (luminescence) of 100, and a standardized neutral density filter (Zeiss neutral density filter 0.5, Carl Zeiss Inc., Thornwood, New York) reduced the luminescence to 50 ± 2. This standardization was carried out daily. Additional fine adjustments were made at the light source before examining each section to compensate for small line voltage changes and drift.

Relative proteoglycan concentrations were determined from staining densities at four sublocations: within the healing defect itself, immediately adjacent to the defect, at the cranial rim of the joint, and 1.5 cm centrad from the defect (Fig. 1). Staining densities at each site were obtained by using the cursor keys of the computer keyboard to draw three rectangles of standard dimensions (10 by 20 pixels) on the digitized video image (Fig. 2). The computer added the luminescence of the pixels within each of the rectangles and then divided by the number of pixels (200) to give an average luminescence between zero and 100. These determinations were made at three depths at each location corresponding to the superficial, middle and deep zones of the uncalcified portion of articular cartilage. The values for proteoglycan concentrations were automatically sorted with respect to origin and stored on a computer floppy disc.

STATISTICAL ANALYSIS OF QUANTITATIVE DATA

The quantitative data were analyzed using a model constructed as a nested (hierarchal) design (13). The data were tested for homoscedasticity and normality. All analyses were performed using the General Linear Model procedure of the Statistical Analysis System (14). The analyses were performed in a hierarchal manner. If an effect was insignificant, it was removed from the model before the next analyses. The following factors were examined for their effect on matrix proteoglycan concentra-

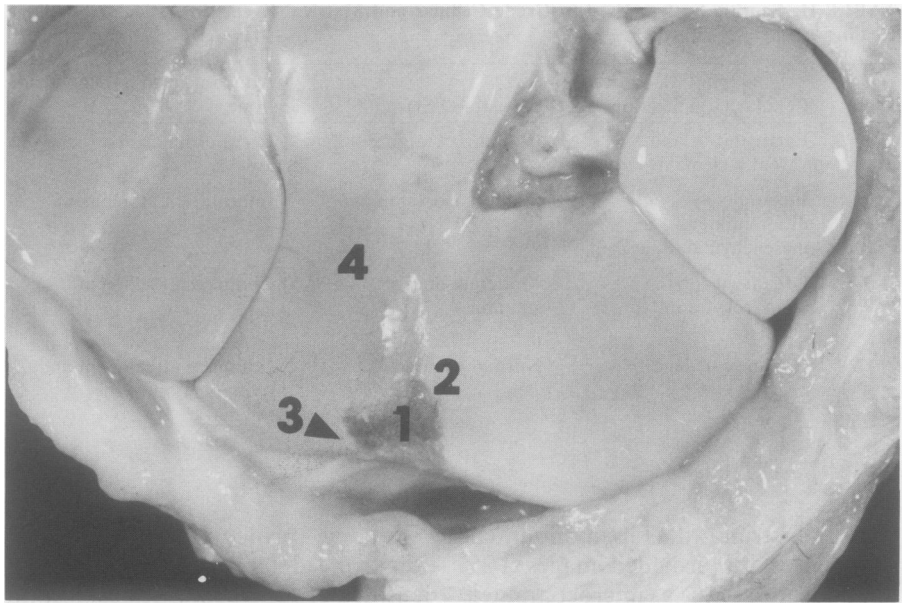

Fig. 1. A small nonweight bearing defect one month after surgery showing the sublocations where microdensitometry recordings were made within the defect (1), adjacent to the defect (2), next to the dorsal rim of the joint (3), centrad and distant from the defect (4).

tions: individual horses, left versus right sided joints, carpal versus stifle joints, weight bearing or nonweight bearing, the lesion size, sublocations within or around the defects.

RESULTS

The horses had mild to moderate hindlimb lameness during the first postoperative day due to periarticular irrigating fluid around the stifle. They maintained an alert attitude and continued to eat well during the first week after surgery, however they did not attempt to trot more than a few steps for approximately five days. Additional postoperative analgesics were not required.

Averaged qualitative scores for the healing defects are shown in Table III. An overall trend is evident showing a gradual increase in cellular organization, matrix staining, and attachment of new repair tissues to subchondral bone over the nine month experimental period.

GROSS PATHOLOGY

Gross examination of the articular defects at one month postoperatively showed little if any changes since surgery. A thin friable opalescent tissue was evident in the defects overlying the yellow subchondral bone. Tongues of cartilage from the lesion's rim extended into three of four of the stifle defects and one of the eight carpal lesions. This changed the original square shape into an irregular trapezoid or triangle.

At two and one-half and four months after surgery there was more obvious evidence of healing especially at the center of the lesions. A more vascular, pink tissue was well adhered to the subchondral bone and covered, but did not fill the defect to the level of the articular surface. Stifle lesions appeared to have thicker, paler and more resilient repair tissues than carpal lesions. Five millimeter square stifle defects had become stellate by 2.5 months and were nearly undetectable fissures by four months (Fig. 3). Repair of all nonweight bearing third carpal bone defects lagged behind other sites, and three out of four of these defects had become larger than the original defect. Poorly attached fibrous tissue and exposed subchon-

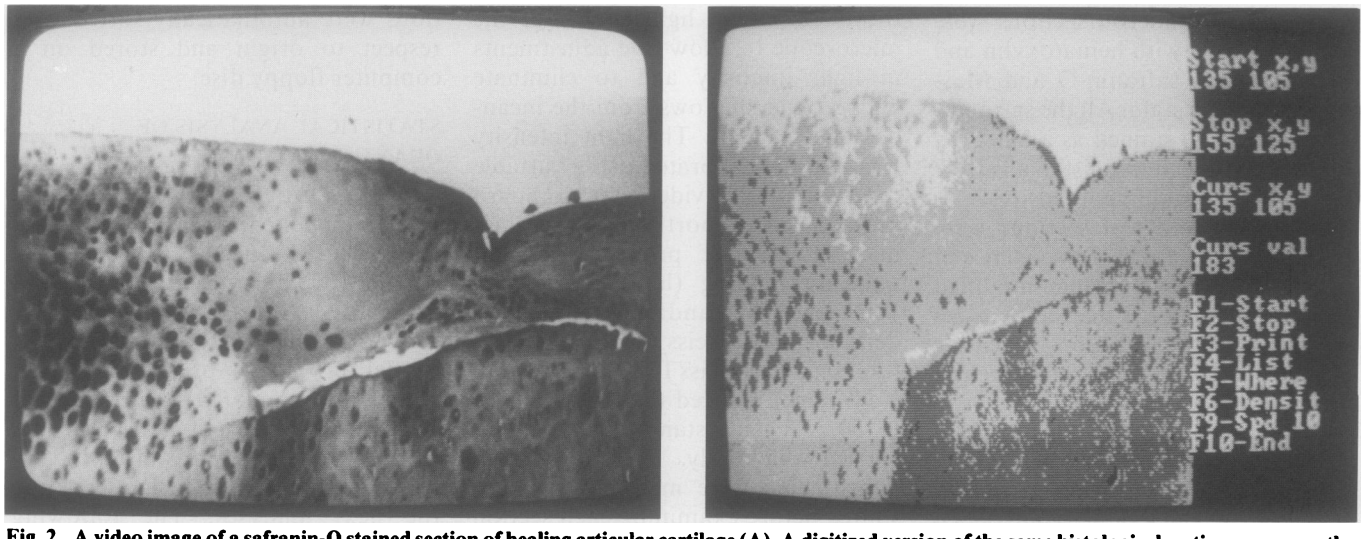

Fig. 2. A video image of a safranin-O stained section of healing articular cartilage (A). A digitized version of the same histological section as seen on the computer screen in eight shades of grey (B). The computer system processed images using more than 100 grey levels. The rectangle (broken lines) outlines one of the standardized sites where staining of articular cartilage was sampled.

TABLE III. Averaged Qualitative Scores for Cartilage Healing in Full Thickness Defects

Time (months)	Mean Score (0-3)	Range
1	0.4	0-1
2.5	0.7	0-2
4	0.6	0-3
5	1.7	1-3
9	2.3	1-3

dral bone was evident in the defects. The cartilage around these lesions was darker and appeared thinner than the joint surface of the second and fourth carpal bones (Fig. 4).

Lesions at five months showed more variability. Small radiocarpal and femoropatellar lesions were reduced to a ripple in the articular surface. The large counterparts of these lesions had dense white connective tissue filling the defect, but the lesions' original outline was still evident. Three of the four large carpal lesions had denuded, roughened surfaces in lieu of repair. These included lesions at the dorsal rim of the middle carpal joint which had well developed synovial adhesions and roughened and disrupted perilesional cartilage.

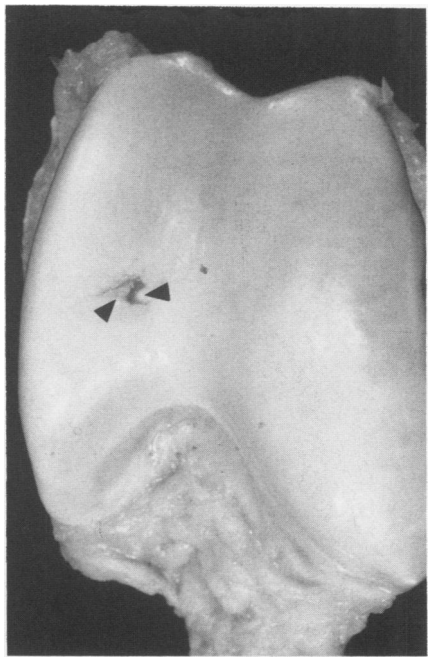

Fig. 3. A small defect within the trochlear groove of the femoropatellar joint at 2.5 months postoperatively. Peninsulas of articular cartilage (arrowheads) extended from the defect's perimeter into the lesion.

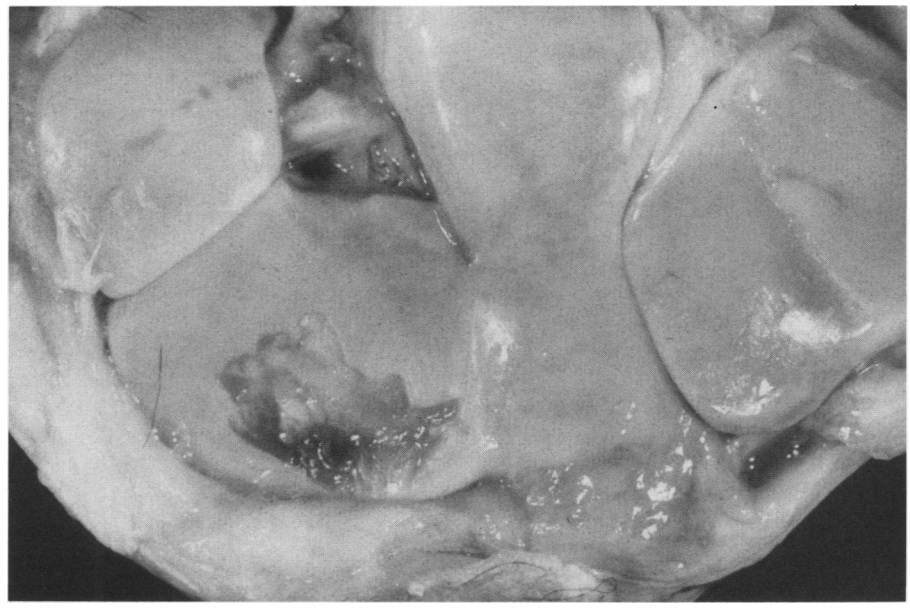

Fig. 4. A nonweight bearing lesion of the third carpal bone that enlarged considerably during a four month postoperative period. Note the dark roughened appearance of the exposed subchondral bone and the hypertrophied synovial membrane attached to the carpal bone's dorsal rim. There was a widespread discoloration of the joint surface.

Repair tissues were at the level of the surrounding articular surface at nine months. All small weight bearing lesions were difficult to find at this time. Large healing lesions were identified by clefts at their perimeter and repair tissues that were somewhat paler than the surrounding articular cartilage (Fig. 5). Two large middle carpal lesions still had incomplete fibrous ingrowth and dark, exposed, subchondral bone.

HISTOPATHOLOGY

Hematoxylin and eosin stained sections showed that extrinsic vascular and mesenchymal proliferation were well established at one month. Swirling groups of mesenchymal cells with large oval pale staining nuclei were the predominant cell type. These cells originated from the subchondral bone and invested the deepest portion of the remaining articular cartilage at the perimeter of the lesion. Masson's trichrome stained sections emphasized the random orientation of collagen fibers throughout the new connective tissue at this time (Fig. 6). Cartilage necrosis adjacent to lesions was frequent and was manifest by small pyknotic chondrocyte nuclei or completely empty chondrocyte lacunae and pale staining matrix (Fig. 7).

Lesions adjacent to the cranial rim of carpal joints had an additional perichondrial response characterized by pannus formation that actively resorbed bone on the cranial face of

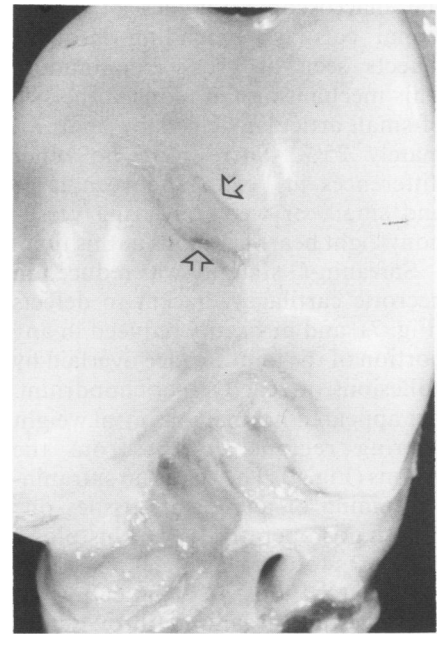

Fig. 5. A large weight bearing lesion in the femoropatellar joint nine months postoperatively. There was an irregular narrow cleft at the lesion's perimeter (arrows).

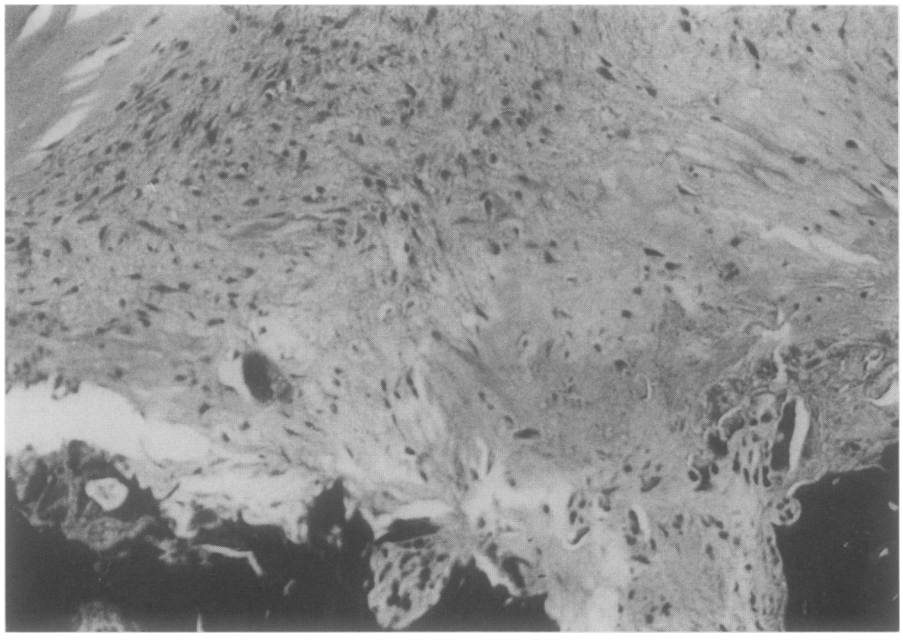

Fig. 6. Young fibroblasts originating from the subchondral bone produced randomly oriented collagen fibers one month postoperatively. Masson's trichrome, original magnification X50.

the radial or third carpal bones (Fig. 8). In these cases, synovial membrane or reactive perichondrium adhered to the defects (Fig. 9). These reactive tissues appeared to contribute vasculature to the healing defect.

In addition to the expected extrinsic repair mechanisms matrix flow was seen in small diameter stifle lesions (Fig. 10). This finding correlated with the macroscopic tongues of perilesional cartilage extending into the defects seen at gross examination. This mechanism had reduced the size of small articular defects by approximately 25%. There were no other differences in healing between large and small, or weight bearing versus nonweight bearing lesions at this time.

Safranin-O staining was reduced in necrotic cartilage adjacent to defects (Fig. 7), and markedly reduced in any portion of the joint surface overlaid by adhesions or reactive perichondrium, but appeared normal in central weight bearing regions distant from the lesions (Fig. 9). There was no safranin-O staining of any repair tissues one month postoperatively. The histological scores for cartilage healing ranged from 0 to 1 out of 3 indicating an overall poorly organized fibrovascular response.

Changes between 2.5 and four months were limited to an increase in the number and organization of trichrome stained collagen fibers in all lesions. These collagen fibers and the nuclei of mature fibroblasts were oriented parallel to the articular surface. Fibrous tissue was incorporating areas of matrix flow into the repair by 2.5 months. The repair tissue became better attached to both the subchondral bone and the perimeter of the lesions by four months. Large blood vessels were evident in the subchondral area beneath the defect where fibrous proliferation, new bone production, and osteoclastic remodelling of bone occurred simultaneously. Matrix flow contributed to the repair process in all stifle lesions, reducing their area by 50 to 90%. They were identifiable only by reduced matrix staining with safranin-O and a thin partial thickness fissure at the articular surface and had near normal cellular constituents and organization (Fig. 10). There were occasionally small areas of calcified cartilage remaining in the defects which were being slowly resorbed by osteoclasts. These areas impaired the incorporation of matrix flow formations into the rest of the repair, often resulting in a cleft (Fig. 7).

Matrix staining with safranin-O was minimal in all repair tissues, and was markedly reduced in areas adjacent to defects at the cranial rim of carpal bones. This was most evident in nonweight bearing carpal defects which were undergoing fibrous replacement of articular cartilage covered by adhesions.

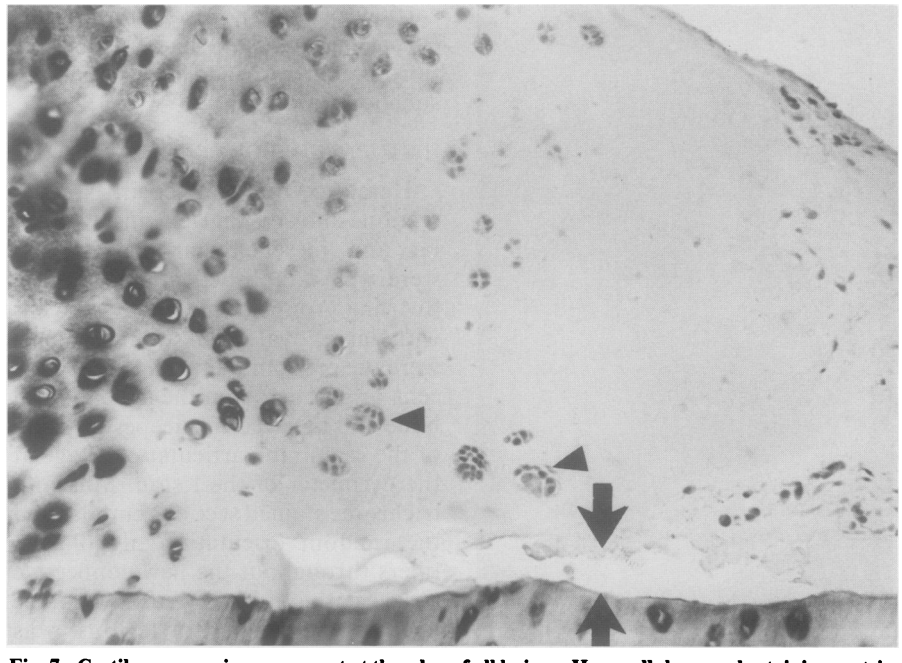

Fig. 7. Cartilage necrosis was present at the edge of all lesions. Hypocellular poorly staining matrix had empty chondrocyte lacunae, and isolated groups of chondrocyte-clones (arrowhead). Note that the degenerate area was poorly attached to the calcified layer of cartilage (arrows). Safranin-O, original magnification X30.

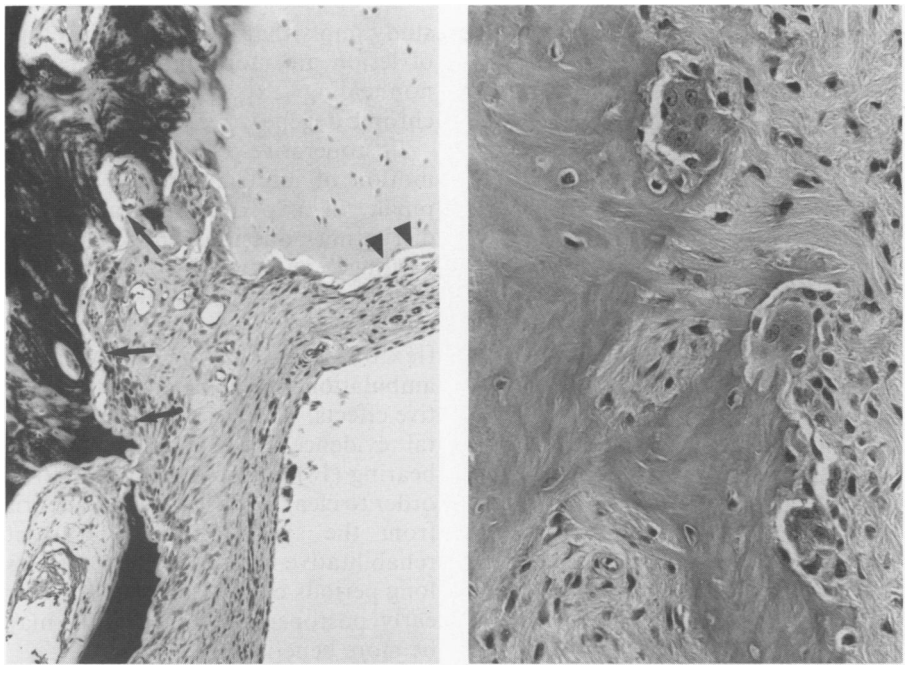

Fig. 8. A proliferative perichondrial reaction resorbed subchondral bone (arrows) and covered the adjacent articular cartilage (arrowheads) (A). Masson's trichrome, original magnification X12.5. Multinucleate osteoclasts within the activated perichondrium destroyed cortical bone and invaded the marrow cavity of the third carpal bone (B). Hematoxylin and eosin, original magnification X30.

At five months after surgery there was a further increase in the amount and organization of dense fibrous tissue which now contained small groups of chondrocytes. All repair tissues, sites near the cranial rim of the third carpal bone, and all perilesional areas continued to demonstrate markedly reduced safranin-O staining compared to uninjured cartilage in central sublocations (Fig. 1). Many large defects had clefts developing between repair tissues and the subchondral bone, and torn strands of connective tissue extending into the joint space.

At nine months there were more areas of plump, dark staining chondrocytes forming typical lacunae, however dense, mature fibrous tissue was still predominant. Three of four middle carpal lesions had some evidence of disruption of the repair tissue at their perimeters. Cleft formation between the repair tissue and subchondral bone resulted in cartilage flaps. In these lesions there was further degeneration of the articular surface at the dorsal rim of the joint and cartilage replacement by dense fibrous tissue.

Matrix staining was improved in and around lesions that had new cartilage formation but was still markedly reduced compared to other undamaged cartilage distant from the lesion. Areas undergoing degeneration at the cranial rim of the joint had little or no matrix staining.

QUANTITATIVE MICRODENSITOMETRY OF SAFRANIN-O STAINED SECTIONS

No statistically significant differences were noted with respect to relative proteoglycan concentrations between individual horses belonging to the same time group, or left versus right joints. Similarly there were no significant overall differences between radiocarpal, middle carpal and femoropatellar joints. The main effects of lesion size and location within the joint could not be separated because of a significant interaction ($p < 0.01$), although significantly higher proteoglycan levels were present in small weight bearing defects ($p < 0.01$, Table IVA). Thus small weight bearing lesions elaborated more proteoglycan during the experimental period when compared to all other lesions. The sublocation adjacent to lesions had much more proteoglycan compared to other sublocations in or around defects ($p < 0.001$, Table IVB). Since a sublocation difference existed, a two way ANOVA was performed to examine sublocation differences

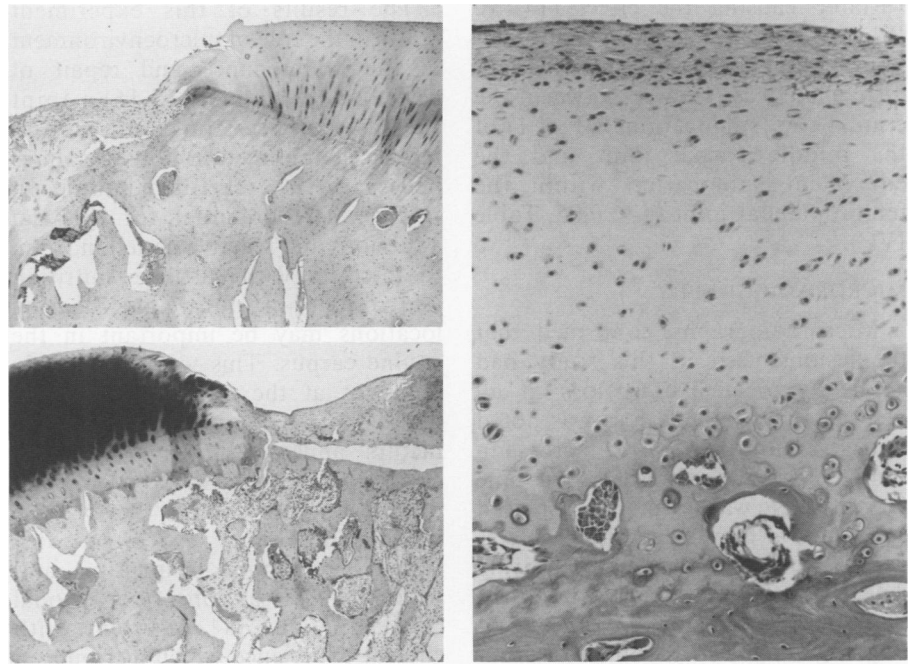

Fig. 9. Cartilage covered by reactive perichondrium had greatly reduced matrix staining (A), compared to cartilage on the central side of the defect which was unaffected by perichondrial reaction or synovial adhesions (B). Higher magnification of matrix loss associated with reactive perichondrium (C). Safranin-O, original magnification X3 (A and B), X12.5 (C).

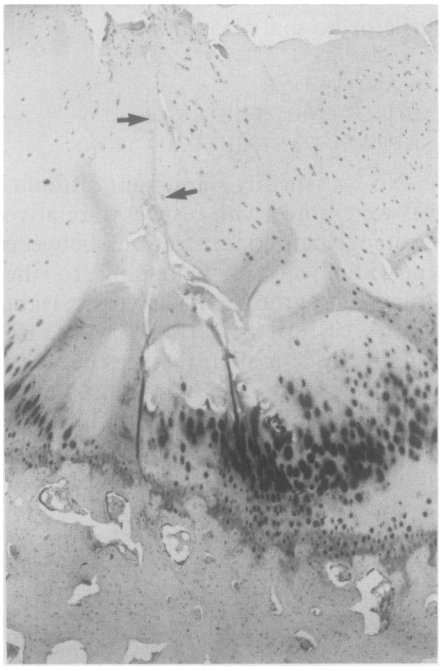

Fig. 10. A narrow fissure (arrows) resulting from matrix flow in a small femoropatellar lesion 2.5 months postoperatively. There was little evidence of extrinisic cartilage repair. The hypocellular cartilage around the defect had markedly reduced matrix staining. Safranin-O, original magnification X30.

within joints. When significant differences were found, Fisher's Significant Difference was used to isolate the variable causing the effect (14,15). When sublocations within different joints were compared, a significant difference was shown between the cranial rim (sublocation 3, Fig. 1) of the middle carpal joint and the equivalent sublocation within the femoropatellar joint ($p < 0.05$, Table IVC).

MICRORADIOGRAPHY

Microradiography confirmed that the lesions used in this study had surgically created bone loss in all defects. Further bone loss was noted until five months when an increase in radiodensity was present. At nine months there was normal to increased subchondral bone beneath all defects except for the nonweight bearing defects of the third carpal bone. In these cases there was evidence of ongoing bony destruction both within the defect and at the cranial rim of the carpal bone. In some cases perichondrial invasion of the dorsal face of the third carpal bone was noted (Fig. 11).

TABLE IVA. Mean Luminescence Value for Each Type of Lesion

Size	Location	Mean Luminescence	SD
Small	Nonweight bearing	51.1	25.2
Small	Weight bearing	42.9[a]	24.8
Large	Nonweight bearing	52.7	29.0
Large	Weight bearing	51.7	27.6

[a]Significantly different at $p < 0.05$

TABLE IVB. Mean Luminescence Value at Each Sublocation

Sublocation	Mean Luminescence	SD
1	58.5	24.2
2	24.4[a]	16.2
3	49.3	23.0
4	70.3	21.0

[a]Significantly different at $p < 0.05$

TABLE IVC. Mean Luminescence Value for Each Joint at Sublocation 2

Joint	Mean Luminescence
Radiocarpal	26.7[a]
Middle carpal	21.6
Femoropatellar	29.4[a]

[a]Significantly different from each other at $p < 0.05$ using the Fisher Significant Difference Test

DISCUSSION

The results of this experiment reaffirm the role of microenvironment in the maintenance and repair of articular cartilage (15,16). Joint surface compression and motion induce the bidirection flow of solutes necessary for cartilage nutrition (16,17). The potential for synovial adhesions and reactive perichondrium to interfere with cartilage nutrition and repair in nonweight bearing locations may be important in the equine carpus. This was particularly apparent at the cranial rim of the middle carpal joint where these two factors appeared to interfere with cartilage homeostasis. Not only did these lesions not heal but they became larger and were associated with subchondral bone resorption and widespread disruption of perilesional cartilage. This is consistent with clinical experience which attributes a poor prognosis to large osteochondral defects of the third carpal bone (Personal communication, (McIlwraith CW, 1986). The findings of this study imply that horses with this type of lesion are more likely to develop nonhealing expansive lesions and chronic degenerative joint disease.

Postoperative continuous passive motion of joints improved articular repair in experimental rabbits by disrupting adhesions and optimizing cartilage nutrition (5). Nonweight bearing continuous passive motion is not possible in the horse but passive flexion and early postoperative ambulation could have similar positive effects. There is other experimental evidence to support early load bearing (18) and joint motion (19) in order to clear hemarthrosis and debris from the synovial cavity. Current rehabilitative regimes for horses stress long periods of boxstall rest, however early postoperative ambulation may be more beneficial.

Part of the aim of this study was to investigate the mechanisms of equine articular repair. Predictably, the horse is like other species and appears to rely to a large extent on extrinsic cartilage healing of full thickness defects. However, the results of this study show that the contribution of matrix flow to equine articular cartilage healing has been underestimated. Matrix flow was noted in all types of lesions, but was most obvious in the stifle where joint cartilage was considerably thicker than in carpal joints. Matrix flow was able to reduce the area of small defects by 50 to 90% within the first 2.5 months by creeping a few millimeters towards the center of the defect. The same degree of matrix flow was probably present in large defects, but its contribution to reducing their area would be considerably less: if matrix flowed 3 mm from the perimeter of all defects centrad, a 5 mm lesion would be reduced by more than 80%. Fifteen millimeter lesions would be reduced in area by a mere 36% requiring a longer period for extrinsic healing to provide the necessary surface. This study confirms previous work showing that small lesions heal readily, while larger lesions have more uncertain outcomes (9).

The reasons for the failure of the horse to produce a lasting joint surface are also of clinical significance. Large (15 mm square) lesions had good initial repairs at 2.5 months postoper-

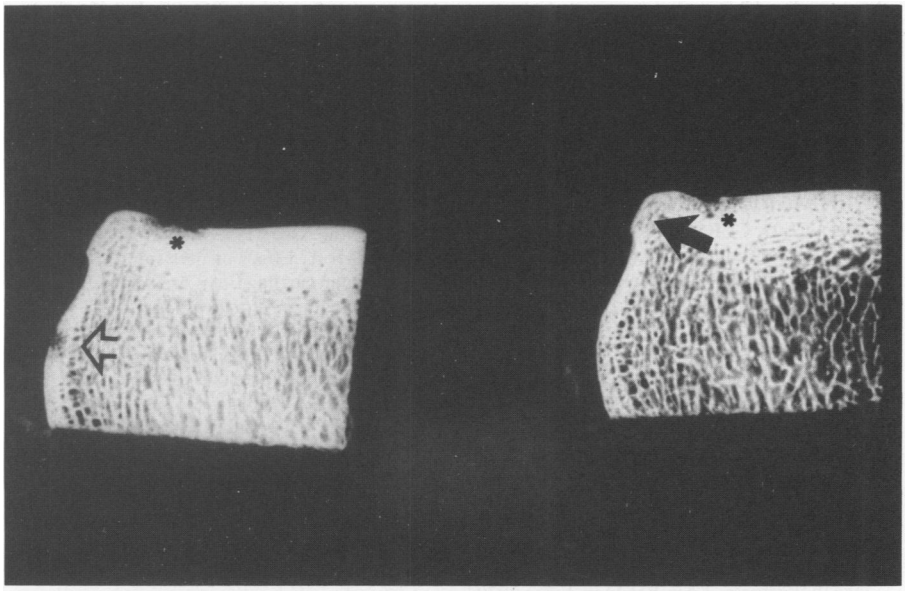

Fig. 11. Thin section microradiography illustrates the surgical defect (*), resorption of bone by perichondrium on the dorsal face (open arrow) and dorsal rim (closed arrow) of the third carpal bone. (Capsular attachments were immediately distal to the area of bone loss on the dorsal face.)

atively, but by five months clefts between the reparative tissue and subchondral bone were common. These clefts became undermined flaps of fibrous tissue which were disrupted by normal biomechanical forces, resulting in exposed subchondral bone. The reason for this is not clear from this study but opposing articular surfaces would be more likely to protrude into large defects, impinging on fragile repair tissues, and result in their disruption. Thus, the unavoidable effect of weight bearing in larger lesions may be detrimental. Larger defects are also likely to liberate more microscopic cartilage particles which have been shown to perpetuate synovitis and impair articular homeostasis in experimental animals (20,21). Despite recent innovations in the treatment of cartilage defects, a poor prognosis for athletic performance is warranted for large, directly load bearing lesions.

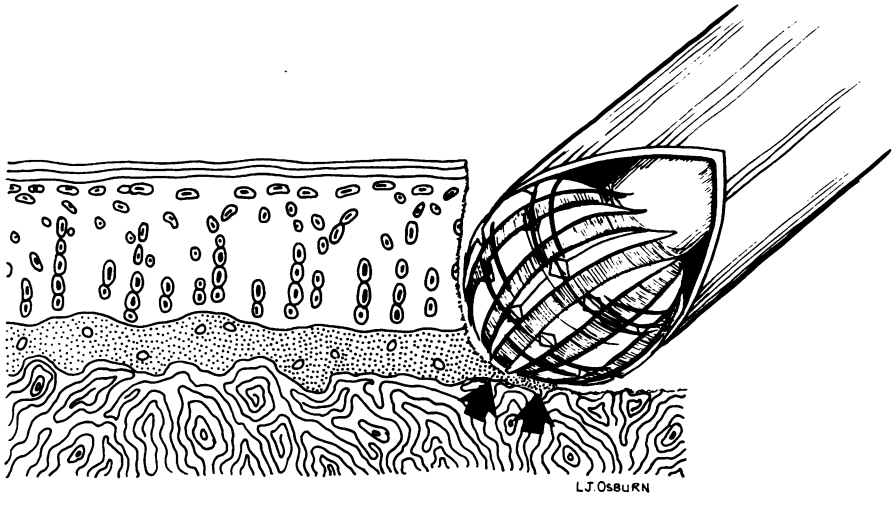

Fig. 12. Use of a motorized arthroplasty burr is unlikely to completely resect the calcified cartilage between the tidemark and subchondral bone. A 1 to 2 mm thick zone of calcified tissue remains which interferes with invasion of extrinsic repair tissues, and their attachment to the subchondral bone.

Lack of attachment of repair tissues to subchondral bone was also present where the layer calcified cartilage had not been removed at surgery. Calcified cartilage appeared to be an effective barrier to invasion of fibrous tissue from the subchondral bone (Figs. 5 and 7). There was both gross and microscopic evidence of incomplete attachment of cartilage flow formations to the subchondral bone at the perimeter of defects. This may represent a weak point in the repair tissues, being responsible for the eventual disruption of some repairs. It implies that surgeons should meticulously remove all calcified cartilage between the tidemark and osteochondral junction when curetting joint surface defects. Motorized burrs are unlikely to achieve this at the perimeter of defects because of their round shape (Fig. 12). A hand instrument such as a small curette would make sure the outline of the defect is perpendicular to the articular surface and devoid of calcified tissue.

Quantitative microdensitometry data suggest another reason for the ultimate failure of cartilage repair. Mean proteoglycan levels in and around defects were still only a fraction (approximately 75%) of those in noninjured articular cartilage at more central sublocations. The fact that there was no significant difference between proteoglycan levels within the repair tissues and around the defects suggests that the hypocellular, poorly staining cartilage remaining at the perimeter of defects is slow to replace its matrix. Since both proteoglycan and collagen are necessary to provide the shear resistance and viscoelasticity of joint surfaces, normal biomechanical loading could result in damage to repair tissues and their subsequent fibrous degeneration and detachment.

These results indicate that matrix proteoglycan levels are increased by nine months, but complete matrix repair has not occurred, leaving collagen fibers unsupported. The advent of arthroscopic surgery has allowed shortened recuperative regimes because the need for soft tissue healing is minimized, however these data show that large or weight bearing lesions are likely to sustain further damage for two reasons. Bony remodelling is incomplete resulting in

poor support of the cartilage surface, and the shear resistant viscoelastic properties of cartilage are dependent on matrix proteoglycans which are still significantly depleted. On the basis of this information, a period of one year's rest from competition should be recommended following surgery for large osteochondral defects, unless more effective rehabilitative regimes are found. However, horses with large lesions at the cranial rim of the third bone are unlikely to benefit from an extended period of rest. Ultimately, they are more likely to have fibrous repair surfaces or exposed subchondral bone.

ACKNOWLEDGMENTS

The authors would like to thank A.M. Trent, J.P. Caron and Joanne Bowen for their contributions to this study.

REFERENCES

1. **GHADIALLY FN.** The Fine Structure of Synovial Joints. London: Butterworths, 1983: 261-306.
2. **FULLER JA, GHADIALLY FN.** Ultrastructural observations on surgically produced partial-thickness defects in articular cartilage. Clin Orthop 1972; 86: 193.
3. **CAMPBELL CJ.** The healing of cartilage defects. Clin Orthop 1969; 64: 54-63.
4. **BAKER B, BECKER RO, SPADARO J.** A study of electrochemical enhancement of articular cartilage repair. Clin Orthop 1974; 102: 251-267.
5. **SALTER RB, SIMONDS DF, MALCOLM BW, RUMBLE EJ, MacMICHAEL D, CLEMENTS ND.** The biological effect of continuous passive motion on the healing of full-thickness defects in articular cartilage. J Bone Joint Surg 1980; 62-A: 1232-1251.
6. **NELSON M, SHEPARD N.** The resurfacing of adult rabbit articular cartilage by multiple perforations through the subchondral bone. J Bone Joint Surg 1976; 58-A: 230-233.
7. **CALANDRUCCIO RA, GILMER WS.** Proliferation, regeneration and repair of articular cartilage in immature animals. J Bone Joint Surg 1969; 64: 54-63.
8. **RIDDLE WE.** Healing of articular cartilage in the horse. J Am Vet Med Assoc 1970; 157: 1471-1479.
9. **CONVERY RF, AKESON WH, KEOWN GH.** The repair of large osteochondral defects. An experimental study in horses. Clin Orthop 1972; 82: 253-262.
10. **KIVIRANTA I, JURVELIN J, TAMMI M, SAAMANEN A-M, HELMINEN HJ.** Microspectrophotometric quantitation of glycosaminoglycans in articular cartilage sections stained with Safranin-O. Histochemistry 1985; 82: 249-255.
11. **KIVIRANTA I, JURVELIN J, TAMMI M, SAAMANEN A-M, HELMINEN HJ.** Fixation, decalcification, and tissue processing effects on articular cartilage proteoglycans. Histochemistry 1984; 80: 569-573.
12. **HURTIG MB, FRETZ PB, NAYLOR J, DOIGE CE.** Accuracy of arthroscopic identification of equine carpal lesions. Vet Surg 1985; 14: 93-98.
13. **FREUND RJ, LITTEL RC.** SAS for Linear Models. Cary, North Carolina: SAS Institute Inc., 1981: 207-220.
14. **CARMER SG, SWANSON MR.** An evaluation of ten pairwise multiple comparison procedures by Monte Carlo methods. J Am Stat Assoc 1973; 68: 66-74.
15. **TRIAS A.** Effect of persistent pressure on articular cartilage. An experimental study. J Bone Joint Surg 1961; 43-B: 376-386.
16. **KINCAID SA, VAN SICKLE DC.** Effects of exercise on the histochemical changes of articular chondrocytes in adult dogs. Am J Vet Res 1982; 43: 1218-1225.
17. **JURVELIN J, KIVIRANTA I, TAMMI M, HELMINEN JH.** Softening of canine articular cartilage after immobilization of the knee joint. Clin Orthop 1986; 207: 246-252.
18. **PALMOSKI MJ, COLYER RA, BRANDT KD.** Joint motion in the absence of normal loading does not maintain normal articular cartilage. Arthritis Rheum 1980; 23: 325.
19. **SALTER RB, BELL RS, KEELEY FW.** The protective effect of continuous passive motion on living articular cartilage in acute septic arthritis. Clin Orthop 1981; 159: 223-247.
20. **EVANS CH, MAZZOCHI RA, NELSON DD, RUBASH HE.** Experimental arthritis induced by intraarticular injection of allogenic cartilaginous particles into rabbit knees. Arthritis Rheum 1984; 27: 200-207.
21. **McILWRAITH CW, FESSLER JF, BLEVINS WE, PAGE EH, REBAR AH, VAN SICKLE DC, COPPOC GL.** Experimentally induced arthritis of the equine carpus: Clinical determinations. J Am Vet Med Assoc 1979; 40: 11-19.